

Functional Expression in Yeast of the Human Secretory Pathway Ca^{2+} , Mn^{2+} -ATPase Defective in Hailey-Hailey Disease*

Received for publication, November 5, 2001, and in revised form, November 29, 2001
Published, JBC Papers in Press, December 6, 2001, DOI 10.1074/jbc.M110612200

Van-Khue Ton, Debjani Mandal‡, Cordelia Vahadj, and Rajini Rao§

From the Department of Physiology, Johns Hopkins University School of Medicine, Baltimore, Maryland 21205

The discovery and biochemical characterization of the secretory pathway Ca^{2+} -ATPase, PMR1, in *Saccharomyces cerevisiae*, has paved the way for identification of PMR1 homologues in many species including rat, *Caenorhabditis elegans*, and *Homo sapiens*. In yeast, PMR1 has been shown to function as a high affinity $\text{Ca}^{2+}/\text{Mn}^{2+}$ pump and has been localized to the Golgi compartment where it is important for protein sorting, processing, and glycosylation. However, little is known about PMR1 homologues in higher organisms. Loss of one functional allele of the human gene, hSPCA1, has been linked to Hailey-Hailey disease, characterized by skin ulceration and improper keratinocyte adhesion. We demonstrate that expression of hSPCA1 in yeast fully complements *pmr1* phenotypes of hypersensitivity to Ca^{2+} chelators and Mn^{2+} toxicity. Similar to PMR1, epitope-tagged hSPCA1 also resides in the Golgi when expressed in yeast or in chinese hamster ovary cells. $^{45}\text{Ca}^{2+}$ transport by hSPCA1 into isolated yeast Golgi vesicles shows an apparent Ca^{2+} affinity of 0.26 μM , is inhibitable by Mn^{2+} , but is thapsigargin-insensitive. In contrast, heterologous expression of vertebrate sarcoplasmic reticulum and plasma membrane Ca^{2+} -ATPases in yeast complement the Ca^{2+} - but not Mn^{2+} -related phenotypes of the *pmr1*-null strain, suggesting that high affinity Mn^{2+} transport is a unique feature of the secretory pathway Ca^{2+} -ATPases.

The best known members of the P-type Ca^{2+} -ATPases are those on the plasma membrane (PMCA)¹ and the sarco/endoplasmic reticulum (SERCA). Their functions and structures have been extensively investigated and characterized over the past several decades. The PMCA is known to extrude Ca^{2+} from the cytosol, whereas the SERCA sequesters Ca^{2+} into the endoplasmic reticulum (reviewed in Refs. 1 and 2). In recent years, a new class of Ca^{2+} -ATPases has emerged, the first member of which was found in the yeast *Saccharomyces cerevisiae* and named PMR1 (for plasma membrane ATPase-related, Ref. 3). PMR1 was localized to the medial-Golgi compart-

ment, a hitherto unusual distribution for a Ca^{2+} pump, where it was found to be important for functioning of the secretory pathway (4–6). These studies showed that cells lacking functional PMR1 exhibit defects in protein glycosylation, processing, sorting, and endoplasmic reticulum-associated protein degradation. In the absence of a SERCA-type Ca^{2+} -ATPase in yeast, PMR1 is the major pump that contributes to the steady-state free Ca^{2+} concentration (10 μM) in the endoplasmic reticulum; this level of Ca^{2+} decreases by 50% in *pmr1*-null mutants (7). Additionally, cytoplasmic Ca^{2+} levels increase up to 16-fold in the *pmr1* mutant (8, 9), despite a compensatory increase in the expression of the vacuolar PMC1 Ca^{2+} pump (9, 10). It is now clear that PMR1 couples ATP hydrolysis to Ca^{2+} transport with an apparent K_m of 70 nM (11, 12).

Intriguingly, PMR1 can also transport Mn^{2+} . The first evidence for a role for PMR1 in Mn^{2+} transport came from the observation that *pmr1* mutants bypass the need for Cu^{2+} superoxide dismutase (SOD1). In a *pmr1sod1* double mutant, Mn^{2+} accumulates in the cytosol at levels 4–5-fold higher than normal and can scavenge harmful free radicals (13). As a trace element, Mn^{2+} is an essential cofactor for enzymes in the cytoplasm (14), mitochondria (15), and Golgi (6). In addition, Mn^{2+} can serve as a surrogate for Ca^{2+} ; thus, in *S. cerevisiae*, a small amount of Mn^{2+} (130 pM) can replace Ca^{2+} (66 nM) to support cell growth (16). On the other hand, high concentrations of cytoplasmic Mn^{2+} are toxic and can interfere with Mg^{2+} binding sites on proteins. It is well known that high Mn^{2+} concentration can compromise the fidelity of DNA polymerases (17). More recently, defective Ty1 retrotransposition in a *pmr1* mutant was shown to be due to Mn^{2+} inhibition of reverse transcriptase.² PMR1 appears to be the principal route for Mn^{2+} detoxification, via the secretory pathway. Maintaining an appropriate level of Mn^{2+} in the Golgi/ER lumen is also equally critical: Mn^{2+} depletion in the *pmr1* mutant leads to defective N-linked and O-linked protein glycosylation. Taken together, these studies illustrate the importance of PMR1 in cytosolic and luminal Mn^{2+} homeostasis.

Research on PMR1 has pioneered the identification of other members of the secretory pathway Ca^{2+} -ATPases. PMR1 shares significant sequence homology with orthologues cloned from diverse organisms including other yeast (18), *Caenorhabditis elegans* (19), and vertebrates, including rat (20), cow (21), and human (22, 23). Recently, heterologous expression of the *C. elegans* PMR1 homologue, ZK256.1, in cultured COS cells has been reported (19) where it was shown to mediate Ca^{2+} and Mn^{2+} transport.

In humans, there exist two PMR1 homologues (gene names *ATP2C1* and *ATP2C2*, protein names abbreviated hSPCA1 and hSPCA2, respectively, in this study). While the tissue distribution of hSPCA2 is not yet known, hSPCA1 is widespread in many tissues including keratinocytes, skeletal muscle, kidney,

* This work was supported by Grant GM62142 from the National Institutes of Health (to R. R.). The costs of publication of this article were defrayed in part by the payment of page charges. This article must therefore be hereby marked "advertisement" in accordance with 18 U.S.C. Section 1734 solely to indicate this fact.

‡ Present address: Indian Inst. of Chemical Biology, 4, Raja S. C. Mullick Road, Jadavpur, Calcutta, 700032 West Bengal, India.

§ To whom correspondence should be addressed. Tel.: 410-955-4732; Fax: 410-955-0461; E-mail: rrao@jhmi.edu.

¹ The abbreviations used are: PMCA, plasma membrane Ca^{2+} -ATPase; BAPTA, bis-(*O*-aminophenoxy)-ethane-*N,N,N',N'*-tetraacetic acid; CHO, chinese hamster ovary cells; HHD, Hailey-Hailey disease; SPCA, secretory pathway Ca^{2+} -ATPase; SERCA, sarco/endoplasmic reticulum Ca^{2+} -ATPase; GFP, green fluorescent protein; MES, 4-morpholineethanesulfonic acid; PBS, phosphate-buffered saline; PMR, plasma membrane ATPase-related; ER, endoplasmic reticulum.

² E. Bolton and J. Boeke, personal communication.

and mammary gland (21, 22). hSPCA1 shares 49% amino acid sequence identity to yeast PMR1, with nearly complete conservation in the transmembrane domains known to be important for transport. Nonsense and missense mutations inactivating one allele of hSPCA1 are found in patients with Hailey-Hailey disease (MIM 16960), whose symptoms involve a loss of keratinocyte cohesion (22, 23). This defect is reminiscent of improper protein glycosylation, sorting, and cell wall morphogenesis in *pmr1*-null mutants (4, 24, 25).

In this study, we present direct biochemical evidence that hSPCA1 is a *bona fide* member of the secretory pathway Ca^{2+} -ATPases. Expressed in yeast and cultured Chinese hamster ovary cells, hSPCA1 localizes exclusively to the Golgi. It complements the *pmr1*-null mutation and transports Ca^{2+} and Mn^{2+} with a high affinity similar to PMR1.

EXPERIMENTAL PROCEDURES

Media, Strains, and Plasmids—Yeast strains were grown in yeast nitrogen base (6.7 g/liter; Difco) supplemented with 2% glucose and necessary amino acids. We used the strain K616 ($\Delta pmr1\Delta pmc1\Delta cnb1$), in which both *PMR1* and *PMC1*, encoding endogenous yeast Ca^{2+} -ATPases, have been disrupted (11, 26). Wild type *PMR1* was reintroduced into this strain as a His-tagged protein expressed from the 2 μ plasmid YE_pHis-PMR1, which has been described elsewhere (27). A similar cloning strategy was employed to insert cDNA of human SPCA1 (KIAA1347; Kazusa Research Institute, Japan) into the expression plasmid pSM1052 (gift of Susan Michaelis, Johns Hopkins School of Medicine). Briefly, a 2.7-kb hSPCA1 PCR product was amplified from a *SalI* and *NotI* insert of KIAA1347 in the plasmid pBluescript II SK⁺ using an *MluI*-containing sense primer (CATCACCATACGCGTATTCCTGTATTGACATCAA; *MluI* site underlined) and a *SacI*-containing antisense primer (GGCGAATTGGAGCTCTCATACTTCAAGAAAAGATGAT; *SacI* site underlined). The hSPCA1 PCR product was cloned into pSM1052 at *MluI* and *SacI* sites, resulting in the introduction of a 9 \times His tag at the extreme N terminus of the protein. To generate the N-terminal GFP-tagged hSPCA1 protein, we introduced *EcoRI* and *SacII* into the hSPCA1 cDNA by a PCR amplification with a sense primer (*EcoRI* site underlined; CGGCCGGAATTCATGATTCCTGTATTGACA) and an antisense primer (*SacII* site underlined; CGCGCCCGCGGTACTTCAAGAAAAGATGATGA). The resulting PCR product was ligated into vector pEGFP-N1 (CLONTECH) at *EcoRI* and *SacII*.

cDNA of the human PMCA4b (GenBankTM accession number AH001521; gift of Adelaida Filoteo and John Penniston, Mayo Clinic, Rochester, MN) was used as a template for PCR with the following sense and antisense primers respectively, GCGCGCACGCGTGGTGATATGACCAACAGC (*MluI* is underlined), and GCGCGCGCGGC-CGCTAAAGCGAGCTCTCCAG (*NotI* is underlined). The product was cloned into pSM1052 at *MluI* and *NotI* sites, resulting in the introduction of the His tag at the extreme N terminus. Plasmid br434 (*CEN PMA1::SERCA1A::ADC1*) expressing rabbit SERCA1 was a generous gift of Dr. Hans Rudolph (University of Stuttgart, Germany) and has been previously described (6).

Phenotype Screens—Growth of K616 yeast cells transformed with plasmids expressing (His)₉-PMR1, (His)₉-hSPCA1, GFP-hSPCA1, rb-SERCA1, or (His)₉-hPMCA4b, was monitored in media supplemented with increasing concentrations of BAPTA and MnCl_2 as in Wei *et al.* (27), with some alterations. BAPTA-supplemented medium was buffered with MES/KOH (final concentration 100 mM) at pH 6.0. 200 μ l of growth medium was inoculated with 0.009 A_{600} units of cells in a 96-well plate and incubated at room temperature for 2–3 days. The cultures were then mixed by gentle vortexing, and growth was measured by determining the absorbance at 600 nm in a SPECTRAMax 340 microplate reader (Molecular Devices). Relative growth was expressed as a fraction of A_{600} of the control culture (no BAPTA or Mn^{2+}).

Membrane Preparation, Gel Electrophoresis, and Antibodies—Sucrose gradient fractionation of yeast cell lysates and total membrane preparation were as described earlier (11), but without the 2-h heat shock. We determined protein concentration with a modified Lowry method (28) after precipitating the protein samples in 10% cold trichloroacetic acid; bovine serum albumin was used as standard (Sigma). Samples were subjected to SDS-PAGE and Western blotting as described (11). His-tagged PMR1, hSPCA1, and hPMCA4b were detected on a Western blot by anti-His₆ antibody (1:5000 dilution; CLONTECH), and anti-rabbit SERCA1 antibody (1:10,000 dilution; Affinity Bioreagent) was used to detect rabbit SERCA1. Horseradish peroxidase-

coupled anti-mouse secondary antibody (Amersham Biosciences, Inc.) was used in conjunction with ECL reagents (Amersham Biosciences, Inc.) to visualize protein bands.

Cell Culture, Transfection, and Confocal Microscopy—Chinese hamster ovary cells were cultured in Ham's F12 medium (Mediatech; Herndon, VA) containing 10% fetal bovine serum (Invitrogen). Cells were grown on 8 chamber glass slides and transiently transfected with either pEGFP-hSPCA1 using LipofectAmine 2000 (Invitrogen) according to the manufacturer's instructions and grown to 70–80% confluency.

For microscopy, GFP-tagged hSPCA1 was visualized in live yeast cells and in transiently transfected CHO cells. Prior to staining with anti-mannosidase antibody, CHO cells were fixed in 2% paraformaldehyde in PBS for 30 min, rinsed with PBS 3 times to remove residual fixative and then permeabilized with 0.5% Triton X-100 in PBS for 15 min. Fixation, permeabilization and all subsequent incubations were at room temperature. Cells were rinsed with PBS three times prior to incubation with 0.1% bovine serum albumin in PBS for 1 h. Next, the permeabilized cells were incubated for 1 h with the primary antibody diluted in PBS containing 0.1% bovine serum albumin at a dilution of 1:1000. The cells were then washed with PBS three times over 30 min and then incubated for 1 h with AlexaFluor 568-labeled goat anti-rabbit antibodies diluted 1:500 in PBS containing 0.1% bovine serum albumin. Finally, cells were again washed with PBS three times over 30 min and then mounted with Prolong antifade mounting medium (Molecular Probes Inc., Eugene, OR). Rabbit anti-mannosidase II antibody was purchased from Dr. Kelley Moremen (University of Georgia; Athens, GA).

$^{45}\text{Ca}^{2+}$ Transport Assays—The transport assay was done as described (11), with modifications. Transport buffer contained 10 mM Hepes/NaOH, pH 6.7, 0.15 M KCl, 5 mM MgCl_2 , 0.5 mM ATP, 5 mM NaN_3 , 500 nM concanamycin A (Sigma), and 10 μ M CCCP (Sigma); $^{45}\text{CaCl}_2$ (22 Ci/g; ICN) was added to 1.7 μ Ci/ml. In $^{45}\text{Ca}^{2+}$ titration assay, the buffer contained 20 μ M CCCP, as well as 15 μ M CaCl_2 and $^{45}\text{CaCl}_2$; EGTA was added in different amounts to titrate free Ca^{2+} concentrations as in Wei *et al.* (29). H_2O used in the buffer was treated with Chelex resin (Sigma) to prevent Ca^{2+} contamination. For other assays, Mn^{2+} or thapsigargin were added to the transport buffer, and the extent of $^{45}\text{Ca}^{2+}$ accumulation in vesicles was measured by liquid scintillation.

RESULTS

hSPCA1 Complements the Phenotype of a Yeast Null Mutant Lacking Known Ca^{2+} Pumps—Phenotype complementation is the first step in establishing that the hitherto uncharacterized human cDNA KIAA1347, defective in Hailey-Hailey disease, is a functional homologue of PMR1. A characteristic phenotype of *pmr1*-null mutants is their dependence on external Ca^{2+} or Mn^{2+} for growth (3). Thus, growth of the host strain K616 ($\Delta pmr1\Delta pmc1\Delta cnb1$) is hypersensitive to divalent cation chelators such as BAPTA or EGTA. Because standard yeast minimal media contain ~100-fold more Ca^{2+} than Mn^{2+} , and the latter is efficiently removed at low chelator concentrations, the observed growth inhibition by BAPTA correlates with Ca^{2+} starvation. Heterologous expression of a high affinity Ca^{2+} pump allows Ca^{2+} to be efficiently scavenged for delivery into the secretory pathway where it is required for protein sorting and modification. Fig. 1 shows that like PMR1, expression of epitope-tagged hSPCA1 can effectively restore BAPTA tolerance to the yeast mutant lacking endogenous Ca^{2+} pumps. Similarly, Mn^{2+} toxicity in K616 is indicative of loss of Mn^{2+} transport. A critical route for Mn^{2+} detoxification is delivery into the secretory pathway via PMR1, and subsequent exit from the cell. Fig. 1 also shows that the hypersensitivity of the *pmr1*-null mutant to Mn^{2+} toxicity can be rescued by introduction of hSPCA1. Strikingly, hSPCA1 confers significantly higher levels of tolerance to Mn^{2+} when compared with PMR1, while BAPTA tolerance typically remained lower. In previous studies we have established that differential sensitivity to BAPTA and Mn^{2+} in PMR1 mutants correlates with altered ion selectivity. The data in Fig. 1 are consistent with the possibility that hSPCA1 is more selective for Mn^{2+} transport, relative to PMR1.

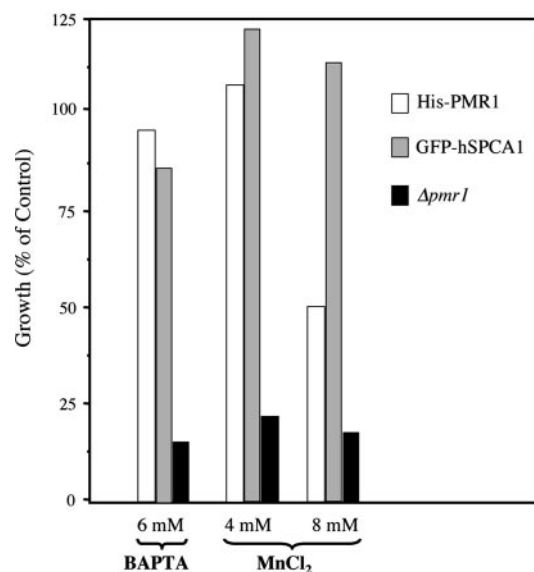


FIG. 1. **hSPCA1 complements $\Delta pmr1$.** Yeast strain K616, carrying the $\Delta pmr1$ mutation, was transformed with plasmid expressing epitope-tagged PMR1 or hSPCA1 and grown in medium supplemented with BAPTA (buffered with 100 mM MES/KOH at pH 6.0), or $MnCl_2$ at the indicated concentrations. Growth (A_{600}) was measured after 48 h at 25 °C and is plotted as percentage of growth in control cultures, un-supplemented with BAPTA or Mn^{2+} . Data are averaged from duplicates, which varied by less than 10%. Similar results were obtained with His-tagged hSPCA1.

hSPCA1 Localizes to the Golgi in Yeast and in Cultured Mammalian Cells—Yeast strains expressing (His)₉-tagged hSPCA1 were grown in 500 ml cultures, lysed gently, and fractionated on a 10-step sucrose gradient. Using an array of organellar markers, we have previously showed that (His)₉-Pmr1 localizes discretely to Golgi fractions, which are separate from endoplasmic reticulum, plasma membrane, and vacuoles (11, 29). Fig. 2A shows that histidine-tagged hSPCA1 localizes to the same fractions as histidine-tagged PMR1, as indicated by the appearance of ATP-driven ^{45}Ca transport activity in fractions corresponding to the Golgi (26 to 30–34% sucrose). The equivalent fractions derived from the vector-transformed host strain were virtually devoid of Ca^{2+} pumping activity. Western analysis of the fractions confirms that hSPCA1 has a distribution similar to that of PMR1 (Fig. 2B).

To determine whether Golgi localization was specific to the secretory pathway Ca^{2+} -ATPases, we examined the distribution of representative members of the SERCA and PMCA subtypes expressed in yeast. Fig. 2 also shows ^{45}Ca transport activity and Western analysis of fractions derived from K616 yeast transformed with plasmid expressing (His)₉-human PMCA4b and untagged rabbit SERCA1. These two Ca^{2+} -ATPases are distributed in the denser half of the sucrose gradient, which has previously been shown to contain both endoplasmic reticulum and plasma membrane fractions (11). Clearly, the Golgi localization and $^{45}Ca^{2+}$ transport activity of hSPCA1 expressed in yeast mirrors that of PMR1, and not those of the PMCA or SERCA pumps.

Live yeast cells transformed with GFP-tagged hSPCA1 were examined by confocal microscopy. Fig. 3 shows that GFP fluorescence resides in scattered, punctate structures characteristic of the appearance of Golgi bodies in yeast, and similar to the previously reported distribution of PMR1 (4). Fig. 4A is a confocal image of a field of live chinese ovary cells transiently transfected with GFP-hSPCA1. The majority of fluorescence has a juxtannuclear distribution, similar to the recently reported distribution of the *C. elegans* PMR1 homologue expressed in COS cells (30). To verify the identity of this compartment, the

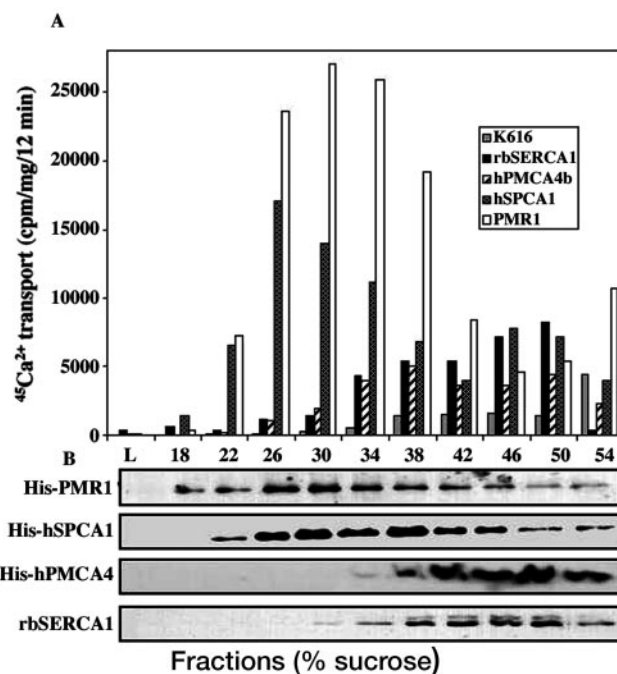


FIG. 2. **Subcellular fractionation of yeast strains expressing Ca^{2+} -ATPases.** A, Ca^{2+} transport activity. K616 yeast expressing His-tagged PMR1, hSPCA1, hPMCA4, or untagged rbSERCA1, respectively, were lysed and fractionated on a 10-step sucrose gradient (18–54% w/w, represented by the numbers 18–54; L, load). All transformed strains exhibited ^{45}Ca transport activity that was clearly distinguishable from the host strain. $^{45}Ca^{2+}$ transport corresponding to the activity of PMR1 and hSPCA1 peaks at 26–34% sucrose, which contain Golgi membranes (11). In contrast, $^{45}Ca^{2+}$ transport activity of hPMCA4 and rbSERCA1 peaks between 38 and 54% sucrose, which contain ER and plasma membranes. B, Western blot. 100 μ g of each sucrose gradient fraction from the experiment shown in panel A was separated by SDS-PAGE, transferred to nitrocellulose membranes, and probed with monoclonal anti-His₉ antibody, or, in the case of rbSERCA1, with anti-rbSERCA1 antibody. Fractions showing immunoreactive bands can be seen to correspond with ^{45}Ca transport activity shown in Panel A.

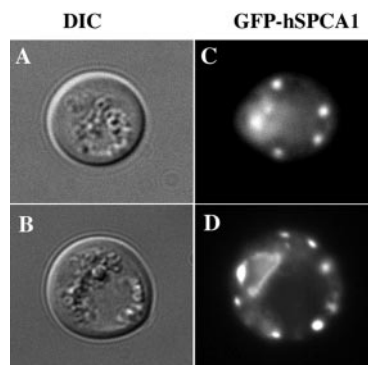


FIG. 3. **Fluorescence microscopy of GFP-tagged hSPCA1 in live yeast cells.** Yeast strain K616, transformed with plasmid expressing GFP-tagged hSPCA1, was examined by confocal microscopy as described under “Experimental Procedures.” Panels A and B are phase-contrast images (DIC) of live cells and Panels C and D show GFP fluorescence. GFP-hSPCA1 appears as punctate vesicular structures scattered in the cytosol.

cells were stained with antibody to the Golgi resident protein, mannosidase II. Fig. 4B shows that GFP fluorescence is essentially superimposable with the signal from mannosidase II, confirming the Golgi localization. These microscopy data, together with subcellular fractionation of yeast membranes, establish that hSPCA1 is a resident Golgi protein, and provide further evidence for classification as a member of the secretory pathway Ca^{2+} -ATPases.

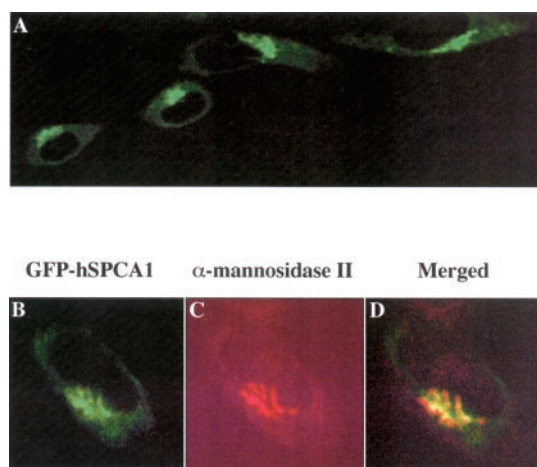


FIG. 4. **Fluorescence microscopy of GFP-tagged hSPCA1 in CHO cells.** Panel A is a field of live CHO cells, transiently transfected with GFP-tagged hSPCA1, showing GFP fluorescence with a juxtanuclear concentration characteristic of Golgi. In Panels B–D, cells were fixed, permeabilized, and treated with antibody against mannosidase II, a resident Golgi marker. GFP fluorescence (Panel B) is superimposable with indirect immunofluorescence from mannosidase II (Panel C), as seen in the merged image (Panel D).

hSPCA1 Transports Ca^{2+} and Mn^{2+} —Vesicles pooled from Golgi-enriched fractions of cells expressing His-hSPCA1 were assayed for $^{45}\text{Ca}^{2+}$ transport activity under conditions that inhibit $\text{H}^+/\text{Ca}^{2+}$ exchange (see “Experimental Procedures”). $^{45}\text{Ca}^{2+}$ transport displayed simple Michaelis-Menten kinetics and was dependent on free Ca^{2+} with an estimated K_m of 260 nM (Fig. 5A). The data are consistent with a single high affinity site for Ca^{2+} , similar to a recently reported value of 250 nM for the PMR1 homologue from *C. elegans* (19). In earlier studies of ^{45}Ca transport and Ca^{2+} -dependent ATPase activity, we have observed a K_m of 70 nM for *S. cerevisiae* PMR1 (11, 29).

The ability of hSPCA1 to bind Mn^{2+} was assessed indirectly by inhibition of $^{45}\text{Ca}^{2+}$ transport, as shown in Fig. 5B. Mn^{2+} inhibition of $^{45}\text{Ca}^{2+}$ accumulation in vesicles decreased with increasing Ca^{2+} concentration, suggesting that the two ions compete for the same sites (not shown). Mn^{2+} inhibition of Ca^{2+} transport activity was significantly greater for the secretory pathway pumps (75–90%) than for human PMCA4 and rabbit SERCA1 (~30%; Fig. 5B, inset).

Thapsigargin, a potent inhibitor of the SERCA pumps, was ineffective in inhibiting Ca^{2+} transport activity of hSPCA1, at concentrations up to 5 μM (not shown). This insensitivity is also exhibited by yeast PMR1 (11) and its *C. elegans* homologue, ZK256.1 (30).

High Affinity Mn^{2+} Transport May be a Unique Property of the Secretory Pathway Ca^{2+} ATPases—To date, there is little evidence that the other P-type Ca^{2+} -ATPases, PMCA and SERCA, can transport Mn^{2+} as effectively as Ca^{2+} . In 1980, Chiesi and Inesi (31) reported a slow accumulation of $^{54}\text{Mn}^{2+}$ in sarcoplasmic reticulum-derived vesicles from rabbit skeletal muscle when Ca^{2+} was absent. In contrast, numerous independent experimental observations have indicated that the secretory pathway homologues of PMR1 from yeast and *C. elegans* can transport Mn^{2+} with high affinity (12, 19, 27, 29). Here, we evaluate Mn^{2+} sequestering activity *in vivo* by comparing phenotypes of yeast strains transformed with plasmids encoding rbSERCA1, hPMCA4 and hSPCA1, respectively. Heterologous expression of all Ca^{2+} -ATPases in the *pmr1*-null mutant restores BAPTA tolerance to levels similar to endogenous yeast PMR1, indicating that all of these pumps share the ability to transport Ca^{2+} (Fig. 6A). In contrast, only the secretory pathway Ca^{2+} -ATPases, hSPCA1 and PMR1, confer toler-

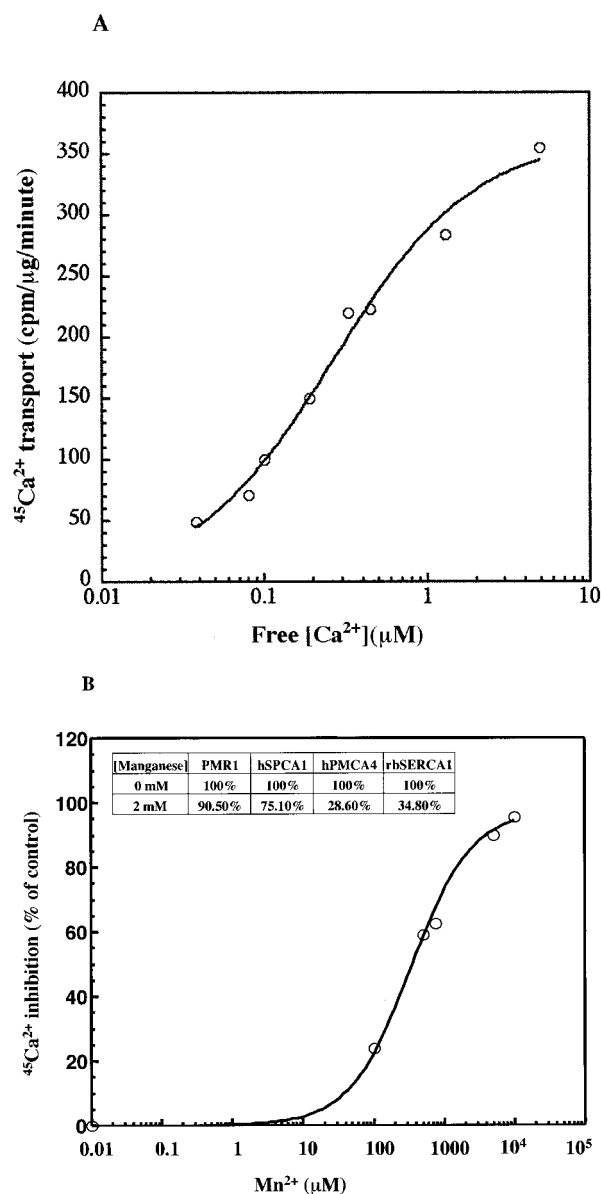


FIG. 5. **Ion transport activity of hSPCA1.** A, $^{45}\text{Ca}^{2+}$ transport. Golgi membranes were pooled from sucrose density gradients of yeast cells expressing His-tagged hSPCA1 and ATP-driven $^{45}\text{Ca}^{2+}$ transport measured as described under “Experimental Procedures.” $^{45}\text{Ca}^{2+}$ (15 μM) was buffered by EGTA and free concentrations calculated according to the MaxChelator software. The data points are averages of duplicate measurements and represent one of two closely similar independent experiments. The line is a best fit to the Michaelis-Menten equation, with an apparent K_m for Ca^{2+} of 260 nM, and an R^2 value of 0.994. B, Mn^{2+} inhibition. $^{45}\text{Ca}^{2+}$ transport activity of hSPCA1 was measured as described in A, except that the total free $^{45}\text{Ca}^{2+}$ concentration was 2 μM , and MnCl_2 was added at the concentrations shown. Data for hSPCA1 were fit to a $K_{0.5}$ of 340 μM . The inset shows inhibition at 0.9 μM $^{45}\text{Ca}^{2+}$ in the presence of 2 mM of MnCl_2 . Peak sucrose density gradient fractions derived from yeast expressing each of the various Ca^{2+} -ATPases indicated were assayed.

ance to high levels of extracellular Mn^{2+} (Fig. 6B). The inability of SERCA and PMCA to confer Mn^{2+} tolerance, taken together with significantly weaker Mn^{2+} inhibition of ^{45}Ca transport (Fig. 5B, inset) suggests a lack of high affinity Mn^{2+} transport activity in these pumps. At this time, however, we cannot exclude the possibility that Golgi localization is somehow critical for effective *in vivo* Mn^{2+} sequestration. Additional evaluation of Mn^{2+} -dependent ATPase activity and phosphoenzyme formation may clarify this issue in the future.

In summary, our current data are consistent with the in-

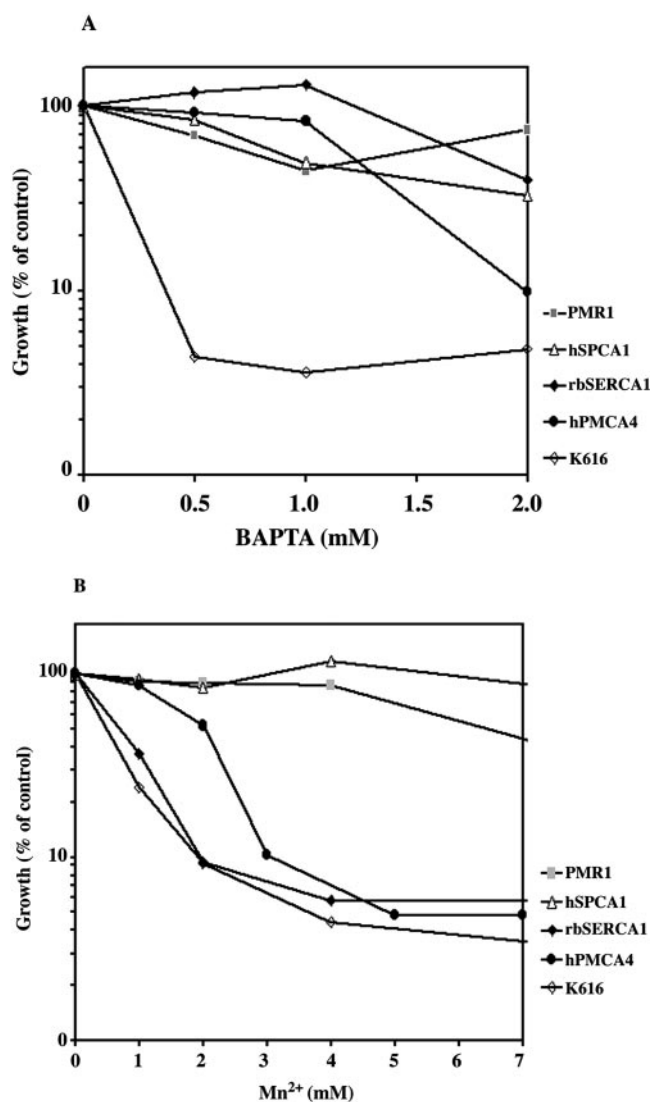


FIG. 6. Differential tolerance to BAPTA and Mn^{2+} in cells expressing hSPCA1, PMR1, hPMCA4, and rbSERCA1. A, all Ca^{2+} -ATPases confer BAPTA tolerance. Yeast strains K616 expressing each of the Ca^{2+} -ATPases shown, were grown in 1 ml of minimal media buffered with 100 mM MES/KOH, pH 6.0, and supplemented with a range of BAPTA concentrations shown. Growth (A_{600}) was monitored after saturation and is displayed as a percentage of A_{600} of the control culture (no BAPTA). B, only the SPCAs confer Mn^{2+} tolerance. Cells were grown as in A, except that the MES buffer was omitted and MnCl_2 was added in place of BAPTA. Only PMR1 and hSPCA1 confer Mn^{2+} tolerance, whereas hPMCA4- and rbSERCA1-expressing cells exhibit a hypersensitivity to Mn^{2+} similar to the $\Delta pmr1$ -null mutant, Lys-616.

triguing possibility that the secretory pathway Ca^{2+} -ATPases have evolved to function as major high affinity Mn^{2+} pumps in the Golgi.

DISCUSSION

In this study we have provided biochemical evidence for the subcellular localization and ion transport properties of an uncharacterized human cDNA KIAA1347, which we have termed the secretory pathway Ca^{2+} -ATPase (SPCA1), in accordance with an earlier proposal by Shull (32). This nomenclature is consistent with the other two well known subtypes of Ca^{2+} pumps, SERCA and PMCA, and serves to distinguish members of a novel and rapidly expanding subtype. We show here that hSPCA1 localizes to the Golgi and mediates the high affinity, thapsigargin-insensitive transport of Ca^{2+} and Mn^{2+} into the secretory pathway, resulting in full complementation of $pmr1$ -

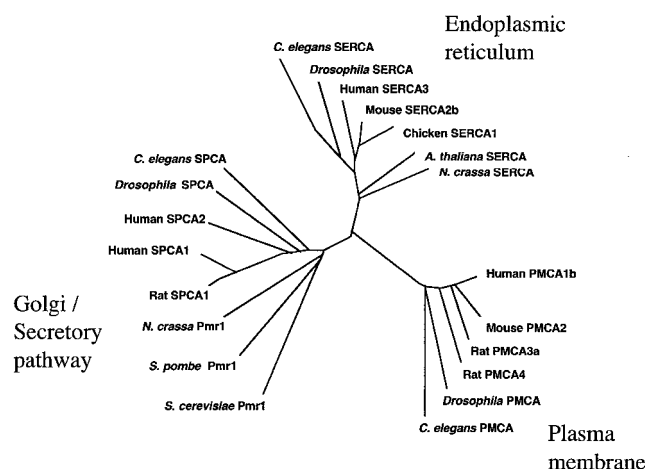


FIG. 7. Phylogenetic analysis of Ca^{2+} -ATPase sequences show clustering of SPCA, SERCA and PMCA subtypes. A selection of Ca^{2+} -ATPase sequences, representing diverse phyla, was aligned using ClustalW 1.5. Phylogenetic analysis was performed using PHYLIP 3.5c and graphic display was done with the DrawTree program. Sequences fall into three distinct clusters representing Ca^{2+} -ATPases of the Golgi/secretory pathway, endoplasmic reticulum, and plasma membrane. PID accession numbers, beginning with *S. cerevisiae* PMR1, are given in clockwise order as follows: 6321271, 3138890, 6688835, 285369, 12644373, 3327220, 7296577, 3875247, 3878521, 7291680, 3211977, 6967017, 114305, 4185855, 6688833, 14286104, 5714364, 111433, 1083756, 7304318, 3549723.

null phenotypes. Phylogenetic analysis of amino acid sequence alignments of representative Ca^{2+} -ATPases from diverse species, depicted in Fig. 7, reveal three distinct clusters of SPCA, SERCA, and PMCA, consistent with non-overlapping organellar distributions and cellular functions.

Haploinsufficiency of hSPCA1, resulting from missense and nonsense mutations in the *ATP2C1* gene, was recently identified in patients with Hailey-Hailey disease (22). In that study, keratinocytes from HHD patients were shown to have higher levels of resting Ca^{2+} , and were defective in removal of excess cytosolic Ca^{2+} despite having intact thapsigargin-sensitive SERCA activity. More recent studies involving heterologous expression of the *C. elegans* PMR1 homologue in cultured COS1 cells demonstrate that the SPCA-filled stores, but not the SERCA-filled stores, are capable of setting up Ca^{2+} oscillations upon stimulation of IP₃ receptors. Thus, defects in spatio-temporal response to Ca^{2+} in HHD may lead to defective Ca^{2+} signaling, gene expression and keratinocyte differentiation. Alternatively, when Ca^{2+} and Mn^{2+} levels are low in the Golgi, secreted or surface proteins may not be correctly glycosylated and sorted, as demonstrated in yeast (6, 24, 25), and may lead to improper keratinocyte adhesion. Our data support the hypothesis that hSPCA1 might play a pivotal role in maintaining cytosolic as well as organellar (particularly Golgi and the secretory pathway) Ca^{2+} and Mn^{2+} concentrations. At present, it remains an important issue to distinguish whether defective cytosolic Ca^{2+} homeostasis, or a deficiency in Golgi Ca^{2+} and Mn^{2+} concentrations is responsible for abnormal keratinocyte adhesion.

The effect of Mn^{2+} on SERCA and PMCA pump activity has been investigated in earlier studies. Mn^{2+} was found to effectively replace Mg^{2+} in promoting ATP hydrolysis (31, 33). In the presence of Mg^{2+} , excess Mn^{2+} competitively inhibited Ca^{2+} pumping activity of rat synaptic vesicles PMCA although no evidence was obtained for $^{54}\text{Mn}^{2+}$ transport (33). Rabbit skeletal muscle SERCA, on the other hand, was shown to bind Mn^{2+} , albeit with an affinity about three orders lower than for Ca^{2+} , and mediate transport at a very slow rate (31, 34). Our data on Mn^{2+} inhibition of ^{45}Ca transport activity of SERCA

and PMCA expressed in yeast are consistent with these earlier observations. In contrast, there is a growing body of evidence on SPCA pumps from yeast, worm and human demonstrating Mn^{2+} tolerant phenotype, Mn^{2+} competition of Ca^{2+} transport, direct assay of ^{54}Mn transport and Mn^{2+} -dependent ATPase activity (12, 19, 27, 29, and this study). Based on these observations, we propose that the SPCA have uniquely evolved as high affinity Mn^{2+} pumps to fulfill physiological roles that are only beginning to be understood.

Acknowledgments—We thank the Kazusa Research Institute (Japan), Susan Michaelis, Kyle Cunningham, Hans Rudolph, John Penniston, and Adelaida Filoteo for generous gifts of plasmids, Kelley Moremen for making available the mannosidase II antibody, and Devrim Pesen for contribution to the sequence alignments.

REFERENCES

1. Strehler, E. E., and Zacharias, D. A. (2001) *Phys. Rev.* **81**, 21–50
2. East, J. M. (2000) *Mol. Membr. Biol.* **17**, 189–200
3. Rudolph, H. K., Antebi, A., Fink, G. R., Buckley, C. M., Dorman, T. E., LeVitre, J., Davidow, L. S., Mao, J. M., and Moir, D. T. (1989) *Cell* **58**, 133–145
4. Antebi, A., and Fink, G. R. (1992) *Mol. Biol. Cell* **3**, 633–654
5. Schröder, S., Schimmöller, F., Singer-Krüger, B., and Riezman, H. (1995) *J. Cell Biol.* **131**, 895–912
6. Dürr, G., Strayle, J., Plemper, R., Elbs, S., Klee, S. K., Catty, P., Wolf, D. H., and Rudolph, H. K. (1998) *Mol. Biol. Cell* **9**, 1149–1162
7. Strayle, J., Pozzan, T., and Rudolph, H. K. (1999) *EMBO J.* **18**, 4733–4743
8. Halachmi, D., and Eilam, Y. (1996) *FEBS Lett.* **392**, 194–200
9. Locke, E. G., Bonilla, M., Liang, L., Takita, Y., and Cunningham K. W. (2000) *Mol. Cell. Biol.* **20**, 6686–6694
10. Marchi, V., Sorin, A., Wei, Y., and Rao, R. (1999) *FEBS Lett.* **454**, 181–186
11. Sorin, A., Rosas, G., and Rao, R. (1997) *J. Biol. Cell* **272**, 9895–9901
12. Mandal, D., Woolf, T., and Rao, R. (2000) *J. Biol. Cell* **273**, 23933–23938
13. Lapinskas, P. J., Cunningham, K. W., Liu, X., Fink, G. R., and Culotta, V. (1995) *Mol. Cell. Biol.* **15**, 1382–1388
14. Cottrell, G. S., Hooper, N. M., and Turner, A. J. (2000) *Biochemistry.* **39**, 15121–15128
15. Hearn, A. S., Stroupe, M. E., Cabelli, D. E., Lepock, J. R., Tainer, J. A., Nick, H. S., and Silverman, D. N. (2001) *Biochemistry.* **40**, 12051–12058
16. Loukin, S., and Kung, C. (1995) *J. Cell Biol.* **131**, 1025–1037
17. Beckman, R. A., Mildvan, A. S., and Loeb, L. A. (1985) *Biochemistry.* **24**, 5810–5817
18. Park, C. S., Kim, J. Y., Crispino, C., Chang, C., and Ryu, D. D. Y. (1998) *Gene (Amst.)* **206**, 107–116
19. Van Baelen, K., Vanoevelen, J., Missiaen, L., Raeymaekers, L., and Wuytack, F. (2001) *J. Biol. Chem.* **276**, 10683–10691
20. Guteski-Hamblin, A.-M., Clarke, D., and Shull, G. E. (1992) *Biochemistry.* **31**, 7600–7608
21. Reinhardt, T. A., and Horst, R. L. (1999) *Am. J. Physiol.* **276**, C796–802
22. Hu, Z., Bonifas, J. M., Beech, J., Bench, G., Shigihara, T., Ogawa, H., Ikeda, S., Mauro, T., and Epstein, E. H. (2000) *Nat. Genet.* **24**, 61–65
23. Sudbrak, R., Brown, J., Dobson-Stone, C., Carter, S., Ramser, J., White, J., Healy, E., Dissanayake, M., Larregue, M., Perrussel, M., Lehrach, H., Munro, C. S., Strachan, T., Burge, S., Hovnanian, A., and Monaco, A. P. (2000) *Hum. Mol. Genet.* **9**, 1131–1140
24. Sohn Y. S., Park, C. S., Lee, S. B., and Ryu, D. D. (1998) *J. Bacteriol.* **180**, 6736–6742
25. Uccelletti, D., Mancini, P., Farina, F., Morrone, S., and Palleschi, C. (1999) *Microbiology.* **145**, 1079–1087
26. Cunningham, K. W., and Fink, G. R. (1996) *Mol. Cell. Biol.* **16**, 2226–2237
27. Wei, Y., Chen, J., Rosas, G., Tompkins, D. A., Holt, A., and Rao, R. (2000) *J. Biol. Chem.* **275**, 23927–23932
28. Lowry, O. H., Rosebrough, N. J., Farr, A. L., and Randall, R. J. (1951) *J. Biol. Chem.* **193**, 265–275
29. Wei, Y., Marchi, V., Wang, R., and Rao, R. (1999) *Biochemistry.* **38**, 14534–14541
30. Missiaen, L., Van Acker, K., Parys, J. B., De Smedt, H., Van Baelen, K., Weidema, A. F., Vanoevelen, J., Raeymaekers, L., Renders, J., Callewaert, G., Rizzuto, R., and Wuytack, F. (2001) *J. Biol. Chem.* **276**, 39161–39170
31. Chiesi, M., and Inesi, G. (1980) *Biochemistry.* **19**, 2912–2918
32. Shull G. E. (2000) *Eur. J. Biochem.* **267**, 5284–5290
33. Low, W., Brawarnick, N., and Rahamimoff, H. (1991) *Biochem. Pharmacol.* **42**, 1537–1543
34. Gomes da Costa, A., and Madeira, V. M. (1986) *Arch. Biochem. Biophys.* **249**, 199–206